

## Chapter 2

# Distance Relaying Algorithm for a Single Line-To-Ground Fault on Single Infeed Transmission Lines

**Abstract** The work presented in this chapter addresses the problems encountered by the conventional digital distance relay used for the protection of transmission lines fed from one end. To observe its behavior during a high resistance single line-to-ground fault, a laboratory prototype of a three-phase transmission line using equivalent power system components has been developed by the authors. Thereafter, a new digital distance relaying algorithm is presented for the compensation of errors produced by the conventional digital distance relay during a high resistance single line-to-ground fault. The proposed algorithm is based on digital computation of impedance, which uses symmetrical components of three-phase currents and voltages measured at the local end only. The proposed algorithm has been tested using MATLAB/SIMULINK (The MathWorks, Natick, Massachusetts, USA) software for a single line-to-ground fault considering wide variations in fault resistance, fault location, power factor, and short-circuit capacity of the source.

**Keywords** Single infeed transmission line • Digital distance relay • High resistance single line-to-ground fault • Symmetrical components • MATLAB

## 2.1 Introduction

Modern power systems involve large amount of investment. An electric power system comprises of generation, transmission, and distribution of electric energy. Growth of power systems has lead to very complex networks extended across large areas. In such situations, the proper functioning of a modern power system is heavily dependent upon the healthy operation of the transmission lines within it. Today's EHV and UHV transmission lines are exposed to treacherous weather. Therefore, they are very likely to be subjected to different types of electrical faults. If the faults are not detected and removed quickly then, in the worst case, they may create instability of the power system, resulting in shut down of either the large parts of the network or the complete network. However, the causes and

consequences of faults can be minimized by operating the power system in a proper way and using sophisticated protective relays.

Digital distance relays are commonly used for the protection of long EHV and UHV transmission lines. Generally, a conventional digital distance relay measures the local end voltages and currents of the transmission line to determine the fault impedance and trips the line if the fault impedance is less than the set impedance. But, for a high resistance single line-to-ground fault, the fault impedance measured by the digital distance relay is not proportional to the impedance of the faulted portion of the transmission line because of the presence of fault resistance in the faulted path. The major problems of fault resistance encountered by the conventional digital distance relay protecting a single infeed transmission line is discussed in this chapter. Afterwards, a new digital distance relaying scheme is proposed to compensate the errors produced by the conventional digital distance relay for high resistance single line-to-ground faults using local end data only. Further, the chapter also includes the detailed analysis of the apparent impedance measured by the conventional digital distance relaying scheme and the proposed scheme for a high resistance single line-to-ground fault considering wide variations in system and fault parameters. Finally, feasibility of the proposed scheme has been tested using MATLAB/SIMULINK software.

## 2.2 Distance Protection of Transmission Lines

Distance protection scheme is normally applied to protect long transmission lines. It acts as the main protection for overhead transmission lines and provides back-up protection to the adjoining parts of the network, such as busbars, generators, transformers, motors, and further feeders. Distance protection is faster and more selective than overcurrent protection. It is also less susceptible to changes in the power system conditions. A further advantage of digital distance protection is that it can be easily adapted for a unit protection scheme, when applied with a communication link [1–4].

Basically, a distance relay determines the impedance of the faulted portion of a transmission line from the measured voltages and currents at the relay location. The measured fault impedance is then compared with the set impedance of the transmission line to be protected. If the measured fault impedance is smaller than the set impedance of the transmission line, it is assumed that a fault exists on the transmission line between the relay and the reach point. This implies that the distance protection in its simplest form can reach to a protection decision with the measured voltage and current at the relay location [1, 2, 4–6].

## 2.3 Stepped Distance Characteristic of a Distance Relay

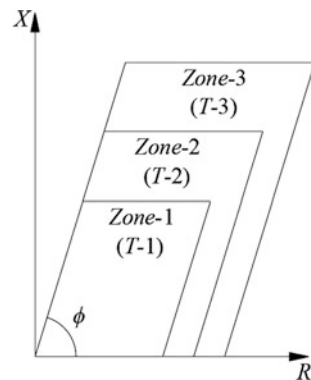
Nowadays, digital distance relays having a quadrilateral characteristic are preferred to protect EHV and UHV transmission lines. In modern digital distance relays, the back-up protection is provided by using stepped distance characteristics. In such a scheme of protection, each distance relay is set for three different zones of protection to protect a specific portion of a transmission system [2, 7, 8]. A typical three-zone quadrilateral characteristic of a digital distance relay is shown in Fig. 2.1. Further, the three zones of protection of the transmission line network are shown in Fig. 2.2.

The first zone or the high-speed zone of a digital distance relay provides main/primary protection to the transmission line to be protected by covering about 80 % of the line length in its first zone and set to operate instantaneously. Adjustment for less than 100 % of the line length is made to avoid overreaching of the relay in the next line section because of transient overreach, errors in the CT's, PT's, and errors in the relay itself. Consequently, a digital distance relay is equipped with another zones (second and third zones), which are set to operate beyond the remote end of the transmission line [2, 5, 6].

The second zone of a digital distance relay covers the complete section of the transmission line to be protected, plus about 50 % of the next line section. Usually, some coordination time delay is provided (about 0.25–0.5 s) for a distance relay to operate in its second zone. Referring to Fig. 2.1, the relay  $R_1$  would operate in the second zone, if the relay  $R_3$  fails to clear a fault occurred just after the relaying point  $R_3$  [2, 5, 6].

The third zone of a digital distance relay encompasses the complete first and second line section. The third zone is coordinated with respect to distance and time with the second zone of the neighboring circuit. Usually, the operating time of a digital distance relay in its third zone is about 0.5–1 s [2, 5, 6].

**Fig. 2.1** Quadrilateral characteristic of a digital distance relay



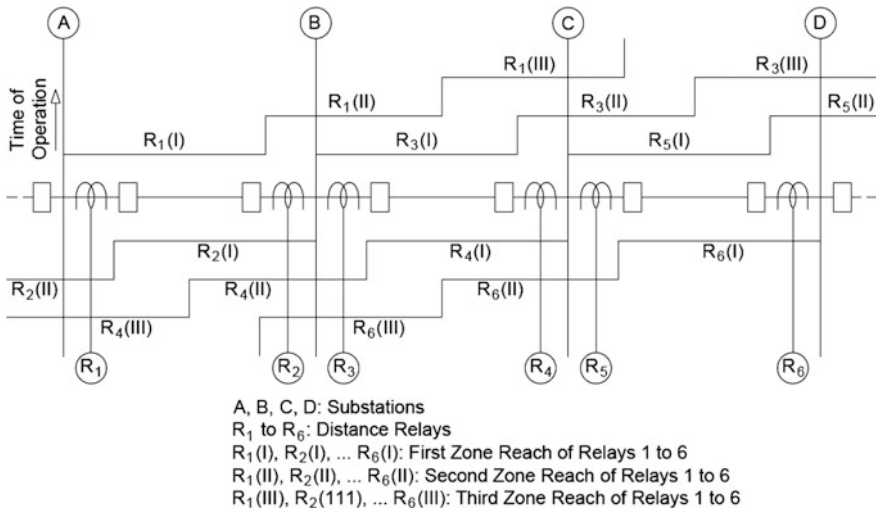


**Fig. 2.2** Stepped distance characteristics of digital distance relays

## 2.4 Problem of Fault Resistance in Distance Protection

In developing a digital distance relay equations, the fault under consideration is assumed to be an ideal (i.e., zero fault resistance) [9–15]. Consequently, the distance relay measures the fault impedance, which is proportional to the length of the transmission line to be protected. But, in reality, the phase and ground faults are seldom solid, i.e., it contains some finite value of fault resistance. In case of a single line-to-ground fault, the fault resistance consists of arc resistance, tower footing resistance, and resistance of ground. While, in case of a line-to-line fault, arc resistance forms the fault resistance. The presence of fault resistance during phase or ground faults introduces an error in the fault distance estimate and may create unreliable operation of a conventional digital distance relay [16]. The most serious cases are:

- Faults in the vicinity of the relaying point in forward/backward direction (close-in faults)
- Faults in the vicinity of the end of protected zone (remote end faults)

If faults involving fault resistance occur at the remote end of the transmission line, the reactance effect appears as the impedance deviation. This can cause mal-operation of a distance relay. During the early periods of an arc, say in the first few milliseconds, the arc resistance is negligible; but as the arc channel gets elongated with time, the arc resistance increases. However, for protective relaying considerations, it is generally assumed that the arc resistance is a constant, given by an empirical formula [17],

$$R_{arc} = \frac{76V^2}{S_{sc}} \quad (2.1)$$

where

$V$  System voltage in kV

$S_{sc}$  Short-circuit kVA at the fault location

The fault resistance introduces an error in the fault distance estimate, and hence, a digital distance relay may underreach/overreach depending upon the remote infeed conditions. The effect of remote infeed current on the fault impedance measurement by a conventional digital distance relay is explained in the next subsection.

## 2.5 Techniques Used in Commercial Relays and Their Problems

Protective relays play a vital role in power systems by minimizing disturbance influence and equipment damage. They detect faults and send trip commands to the appropriate circuit breakers (CBs) to disconnect the faulted zone from the rest of the system. Most of the transmission system protection relays have been designed with distance protection. By measuring the impedance, it can be determined whether the line to be protected is faulted or not [12, 14, 18, 19]. Although the fundamental principle was stated many years ago [14], the distance protection still attracts investigation in theoretical principles as well as in practical applications.

The presence of fault resistance introduces an error in the distance estimation obtained with traditional distance relays, since in resistive faults, the distance between the relay and the fault is not necessarily proportional to the impedance seen by the relay [2, 20]. The problem is further complicated by the influence of pre-fault load current (export or import of power) and by the wide range of fault conditions which may arise in practice [21]. Much research has been conducted to analyze the effect of fault resistance on distance relays [22–24], and several types of distance relay characteristics or algorithms were put forward to eliminate this disadvantage and to improve the resistive tolerance of the distance relays [20, 25]. Theoretically, reactance relays are immune to fault resistance. However, the reactance relay characteristic is often kept inclined upward or downward to prevent overreaching/underreaching of the relay.

Many papers have been published in literature on computer-aided protection of distance relays [12, 26–28], investigating on problems related to the application of different techniques to improve the protection philosophy [29–35]. Several papers have been published in recent years on fault location procedures for high voltage lines [15, 36–40]. Sachdev and Agarwal [38] have presented a new approach, in which they used data from local end and remote end to calculate the fault impedance. Their procedure should result in a precise estimate of fault location, but

appreciable errors are reported for certain locations. Other schemes [15, 36, 37, 39, 40] rely only on the use of local relaying signals and thus enjoy the advantage of not requiring a data link. However, some of these schemes leave certain issues unresolved [21]. Takagi et al. [41] presented a new fault location algorithm for EHV/UHV transmission lines based on distributed parameter model, which assumes the fault path is resistive. The fault location function was given with a nonlinear equation, and the iterative solution technique is needed for obtaining the fault location.

Eissa [20] suggested fault resistance compensation scheme for a ground distance relay at the sending end of a transmission line. Although it has largely avoided underreach, the method may increase the risk of overreach because the fault path resistance is estimated according to the real power measured at the sending end, which includes the load effect. An alternative technique is presented by Richardson et al. [42], in which, the faults are located by comparing voltages and currents at one local end of the transmission line using an optimization procedure. The method has great potential but needs an accurate model of the network and requires iterative calculations.

## 2.6 Current State of the Art

In order to increase the precision in the fault distance measurement and to improve efficiency of the distance relaying scheme for high resistance ground faults, a fault resistance compensation algorithm based on phase coordinates is presented by Filomena et al. [43]. This algorithm uses sending end voltage and current data in an iterative process. However, proper functioning of the said scheme depends on initial estimate of the load current. Further, it is tested for short transmission line only. Zhizhe et al. [44] presented an adaptive digital distance relaying scheme, in which, the operating characteristic boundary of the relay is modified adaptively to minimize the adverse effect of fault resistance. Subsequently, an adaptive relaying scheme for stand-alone digital distance relay has been proposed by Xia et al. [45], in which, the relay settings are renewed automatically according to the changes in power system network configurations using pre-fault data. However, the above two methods are little bit complex. Moreover, these two adaptive schemes may not give satisfactory results during wide variations in system and fault parameters. Thereafter, Jongepier et al. [46] presented an adaptive distance relaying scheme for double circuit lines, in which, the zero-sequence Thevenin impedances of two ends of the line were estimated in order to achieve the correct operation of the distance relaying scheme. However, a prime limitation of the said scheme is that it requires extra measuring equipments to perform the protection duty. Afterwards, Eissa et al. [12] proposed a compensation method based on fault resistance calculation for two-terminal transmission lines. But, the fault resistance calculation relies only on the active power; whereas the effect of reactive power has not been considered by the said scheme.

Bhalja et al. [47] presented a radial basis function neural network-based adaptive distance relaying scheme for different configurations of the transmission lines. But, a major drawback of this scheme is that the neural network requires an extensive training effort for high-quality performance, particularly during wide variations in system and fault parameters. In order to enhance the capability of the distance relaying scheme against fault resistance, Liu et al. [48] presented an adaptive distance relaying scheme based on composite polarizing voltage and using memorized pre-fault and post-fault voltages. However, a correct estimation of the compensated voltage cannot be assured during wide variations in fault parameters. Consequently, very few researchers analyzed the said problems with actual physical implementations.

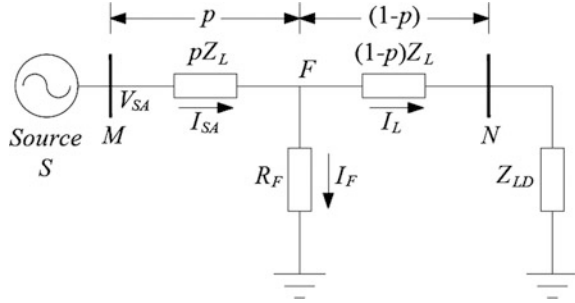
Hence, an attempt has been made in this thesis to observe the behavior of the conventional digital distance relay in the laboratory environment considering a high resistance single line-to-ground fault. The discussions are supported by the experimental validation in the laboratory environment; along with their comparative evaluation by simulation results obtained using MATLAB/SIMULINK software. At the end, a new digital distance relaying algorithm has been proposed to solve different problems faced by the conventional digital distance relay. The performance of the proposed algorithm has been evaluated for different fault and system parameters. It has been observed that the proposed algorithm is highly sensitive toward high resistance faults. Furthermore, it provides satisfactory operation in case of close-in faults during which the conventional scheme fails to operate. Moreover, the proposed algorithm provides effective discrimination between remote end in-zone and out-zones faults.

## 2.7 Performance of the Conventional Digital Distance Relay

In order to check the performance of the conventional digital relaying scheme and the proposed algorithm during a high resistance single line-to-ground fault, model of transmission line network, as shown in Fig. 2.3, is considered. It consists of a source  $S$ , a transmission line connected between buses  $M$  and  $N$ , and a load ( $Z_{LD}$ ). The transmission line is protected by the conventional digital distance relay connected at bus  $M$ . It is assumed that a single line-to-ground fault has occurred at  $p$  percentage of the line length from bus  $M$ .

Throughout the entire discussion,  $Z_L$ ,  $R_L$ , and  $X_L$  represent impedance, resistance, and reactance of complete section of the transmission line, respectively.  $Z_{act}$ ,  $R_{act}$ , and  $X_{act}$  represent actual impedance, resistance, and reactance of the faulted portion of the transmission line, respectively. Further,  $Z_{SA}$ ,  $R_{SA}$ , and  $X_{SA}$  represent apparent impedance, resistance, and reactance measured at the relaying point  $M$ , respectively. Furthermore, the positive-, negative- and zero-sequence components are denoted by subscripts 1, 2, and 0, respectively. Moreover, the positive- and

**Fig. 2.3** Power system model for a high resistance single line-to-ground fault



negative-sequence impedances of the transmission line are assumed to be equal for a single line-to-ground fault [19].

Considering a single line-to-ground fault with fault resistance ( $R_F$ ) occurred at  $p$  percentage of the line length, as shown in Fig. 2.3, the apparent impedance ( $Z_{SA}$ ) measured by the conventional digital distance relay is expressed as follows [8, 49]:

$$Z_{SA} = \frac{V_{SA}}{I_{SA} + 3(k_0 \times I_{S0})} = pZ_{L1} + Z_F = Z_{act} + Z_F \quad (2.2)$$

where

$$k_0 = \left( \frac{Z_{L0} - Z_{L1}}{3Z_{L1}} \right) \text{ and } Z_F = \frac{I_F \times R_F}{I_{SA} + 3(k_0 \times I_{S0})}$$

The first term in the right side of Eq. (2.2) represents actual impedance ( $Z_{act}$ ) of the faulted portion of the transmission line. Conversely, the second term ( $Z_F$ ) represents the adverse effect of the fault resistance that is inherently present in the measurement of apparent impedance by the conventional digital distance relay. Further, the second term clearly indicates that the error produced in the measurement of the fault impedance depends on many parameters, such as fault resistance ( $R_F$ ), sending end current ( $I_{SA}$ ), fault current ( $I_F$ ), as well as, line and ground impedances.

Figures 2.4 and 2.5 represent apparent impedance ( $Z_{SA}$ ) measured by the conventional digital distance relay in case of a high resistance single line-to-ground fault occurred at  $p$  percentage of the line length for no-load and load conditions, respectively.

It has been observed from Fig. 2.4 that, during no-load condition, the conventional digital distance relay measures the correct value of inductive reactance of the faulted portion of the transmission line for a high resistance single line-to-ground fault, i.e.,  $X_{SA} = X_{act}$ . Further, apparent inductive reactance measured by the conventional digital distance relay is not affected by fault resistance present in the faulted ground path. However, referring to Fig. 2.5, it has been observed that when the transmission line is delivering power to a load ( $Z_{LD}$ ), the apparent inductive reactance ( $X_{SA}$ ) measured by the conventional digital distance relay is higher than



**Fig. 2.4** Apparent impedance measured by the conventional relay at no-load

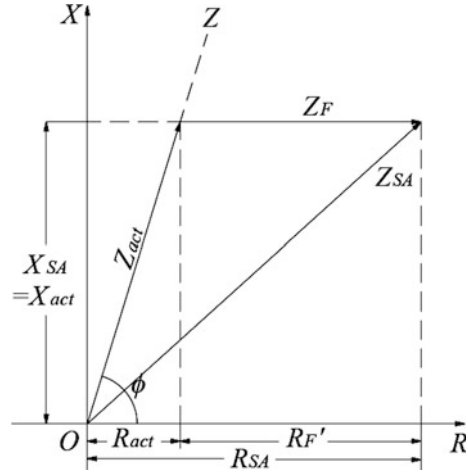
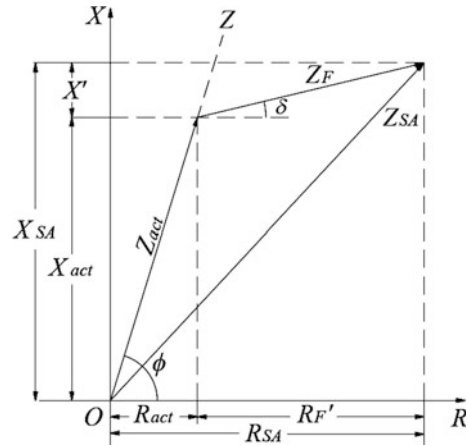


**Fig. 2.5** Apparent impedance measured by the conventional relay with load



the actual inductive reactance ( $X_{act}$ ) of faulted portion of the transmission line, i.e.,  $X_{SA} = X_{act} + X'$  [50]. This is because of the loading effect of the transmission line. Hence, appropriate compensation is required to measure actual impedance ( $Z_{act}$ ) of the faulted portion of the transmission line.

## 2.8 New Digital Distance Relaying Algorithm

Referring to Fig. 2.3, for a single line-to-ground fault, as the symmetrical components ( $I_{F1}$ ,  $I_{F2}$ , and  $I_{F0}$ ) of the fault current ( $I_F$ ) are same, i.e.,  $I_{F1} = I_{F2} = I_{F0}$ ;  $I_F$  can be represented by Eq. (2.3) as follows:

$$I_F = I_{F1} + I_{F2} + I_{F0} = 3 \times I_{F2} \quad (2.3)$$

During a single line-to-ground fault, the positive-sequence reactance increases quickly from sub-transient to synchronous limit after the inception of fault. Conversely, the negative-sequence reactance of a generator remains constant. This assumption is sufficiently accurate to analyze the response of high-speed digital distance relays [51]. Moreover, due to relatively slow response of the generator regulating system compared to the quick response of high-speed distance relay during fault; the load current can be assumed to be unchanged, i.e., it is nearly same as that of its pre-fault value. Therefore, practically, almost the entire unbalanced current (negative-sequence fault current,  $I_{F2}$ ) will pass through the faulted path. Hence, for a single line-to-ground fault, the negative-sequence component of fault current ( $I_{F2}$ ) can be approximated by the negative-sequence component of source current ( $I_{S2}$ ) measured at the relaying point. As the algorithm based on negative-sequence current approximation provides the best accuracy [36], the fault current ( $I_F$ ) is determined by Eq. (2.4) as follows:

$$I_F = 3 \times I_{F2} = 3 \times I_{S2} \quad (2.4)$$

As the faulted phase current ( $I_{SA}$ ) is measured at the relaying point and the fault current ( $I_F$ ) is obtained from Eq. (2.4), the load current ( $I_L$ ) can be expressed as follows:

$$I_L = I_{SA} - I_F \quad (2.5)$$

The load current ( $I_L$ ) and the faulted phase current ( $I_{SA}$ ) can be expressed as follows:

$$I_L = I_L \angle \theta_L = (I_L \cos \theta_L) + j \times (I_L \sin \theta_L) \quad (2.6)$$

$$I_{SA} = I_{SA} \angle \theta_{SA} = (I_{SA} \cos \theta_{SA}) + j \times (I_{SA} \sin \theta_{SA}) \quad (2.7)$$

As the fault current ( $I_F$ ) passes through a fault resistance ( $R_F$ ); it contains the real component of current only. Therefore, the fault current ( $I_F$ ) is given by,

$$I_F = I_F \angle \theta_F = (I_F \cos \theta_F) + j \times (I_F \sin \theta_F) = I_F \cos \theta_F \quad (2.8)$$

Referring to Figs. 2.3 and 2.4, it can be concluded that, during no-load condition, the actual resistance ( $R_{act}$ ) and inductive reactance ( $X_{act}$ ) measured by the conventional digital distance relay depends on the active and reactive components of source current, i.e., ( $I_L \cos \theta_L$ ) and ( $I_L \sin \theta_L$ ), respectively. Similarly, the fault impedance ( $Z_F$ ) measured by the conventional digital distance relay depends on the real component of fault current ( $I_F \cos \theta_F$ ).

Consequently, referring to Figs. 2.3 and 2.5, it can be concluded that, when the transmission line is delivering power to the load,  $R'_F$  measured by the conventional digital distance relay depends on the real components of fault current and load current, i.e., ( $I_F \cos \theta_F$ ) and ( $I_L \cos \theta_L$ ). Whereas,  $X'$  measured by the conventional

digital distance relay depends on the imaginary component of the load current, i.e.,  $(I_L \sin \theta_L)$ .

The final conclusion of the above discussion is that, the magnitude of  $X_{\text{act}}$  and  $X'$  depends on the imaginary components of the source current and the load current, i.e.,  $(I_{SA} \sin \theta_{SA})$  and  $(I_L \sin \theta_L)$ , respectively. Therefore, the magnitude of  $X'$  with respect to  $X_{\text{act}}$  can be represented in terms of the contribution of the imaginary component of load current  $(I_L \sin \theta_L)$  and the imaginary component of source current  $(I_{SA} \sin \theta_{SA})$  measured at the relaying point. This is given by Eq. (2.9) as follows:

$$X' = X_{\text{act}} \times \left( \frac{I_L \sin \theta_L}{I_{SA} \sin \theta_{SA}} \right) \quad (2.9)$$

In Eq. (2.9), the term  $\left( \frac{I_L \sin \theta_L}{I_{SA} \sin \theta_{SA}} \right)$  indicates reactive effect of the load current on reactive part of the source current. Hence, using the value of  $X'$  given by Eq. (2.9), the apparent inductive reactance ( $X_{SA}$ ) measured at the relaying point ( $M$ ) is expressed as follows:

$$X_{SA} = X_{\text{act}} + X' = X_{\text{act}} \times \left( 1 + \frac{I_L \sin \theta_L}{I_{SA} \sin \theta_{SA}} \right) \quad (2.10)$$

Therefore, to measure actual inductive reactance ( $X_{\text{act}}$ ) of the faulted portion of the transmission line, apparent reactance ( $X_{SA}$ ) measured at the relaying point is divided by the term  $\left( 1 + \frac{I_L \sin \theta_L}{I_{SA} \sin \theta_{SA}} \right)$  and it is given by Eq. (2.11) as follows:

$$X_{\text{act}} = \frac{X_{SA}}{\left( 1 + \frac{I_L \sin \theta_L}{I_{SA} \sin \theta_{SA}} \right)} \quad (2.11)$$

It is well known that the ratio of reactance ( $X_L$ ) to resistance ( $R_L$ ) of the transmission line remains constant. Therefore, using the value of ( $X_{\text{act}}$ ) given by Eq. (2.11), the actual value of resistance ( $R_{\text{act}}$ ) of the faulted portion of the line is expressed as follows [52]:

$$R_{\text{act}} = X_{\text{act}} \times \frac{R_L}{X_L} \quad (2.12)$$

## 2.9 Experimental Test Setup

In order to check the behavior of the conventional digital distance relay for a high resistance single line-to-ground fault, a prototype of three-phase transmission line network has been developed in the laboratory environment.

### 2.9.1 Development of Experimental Test Setup

Figure 2.6 shows a power circuit of the experimental test setup. A three-phase power supply is provided to the power circuit through a continuously variable three-phase autotransformer (415 V, 15 A). Many rheostats (18  $\Omega$ , 12 A, with smooth variation of resistance) and inductors (100 mH, 5 A, in steps of 25 mH) are used to make a practical model of a transmission line. A three-phase load bank (415 V, 6 kW) in conjunction with variable inductors is connected at the receiving end of the transmission line. A conventional digital distance relay is connected to the secondary sides of CTs and PTs of ratings 10/5 A and 220/110 V, respectively. A smooth variable rheostat of 350  $\Omega$  is used to develop a high resistance single line-to-ground fault. The circuit parameters are given in Appendix A.

Figure 2.7 shows a control circuit of the test setup, in which, a single-phase autotransformer (230 V, 8 A) is used to provide an auxiliary power supply to the relay and to the control circuit. Three push buttons namely,  $PB_1$ ,  $PB_2$ , and  $PB_3$  are used to make the power circuit ON, OFF, and RESET, respectively. Three neon bulbs indicate status (ON, OFF, and TRIP) of the power circuit. A contactor (C) (which simulates a circuit breaker) is used to connect or disconnect a three-phase power supply to the power circuit using four contacts (C-1 to C-4). Further, two contacts C-6 and C-7 of the same contactor are used to provide ON and OFF indication, respectively. An auxiliary relay (A) is used to trip the contactor and to provide TRIP indication.

Figure 2.8 shows an actual photograph of the laboratory prototype of a transmission line. It is used to analyze the behavior of the conventional digital distance relay during high resistance single line-to-ground faults.

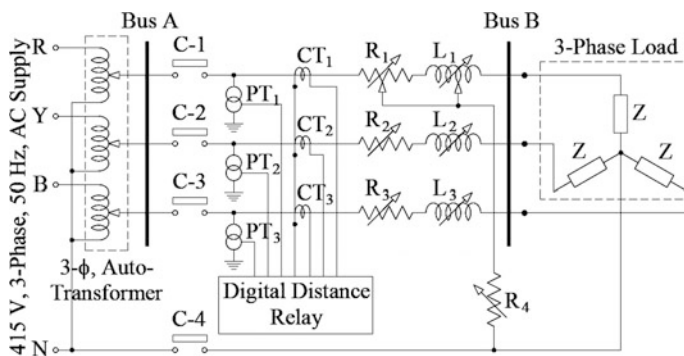


Fig. 2.6 Power circuit of the experimental setup

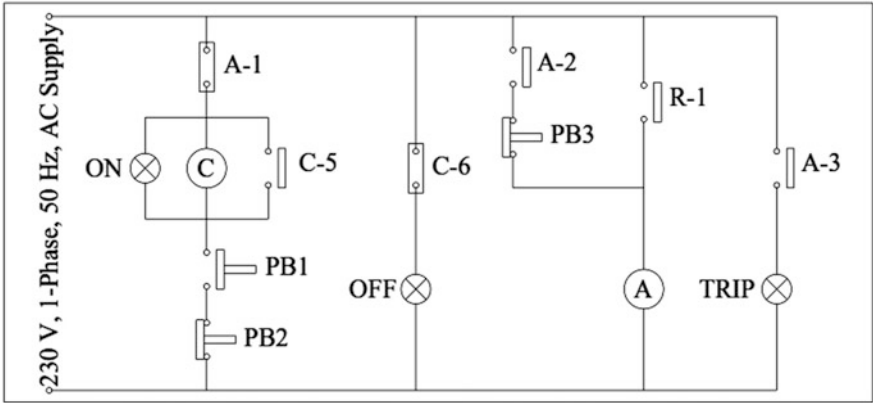


Fig. 2.7 Control circuit of the experimental setup

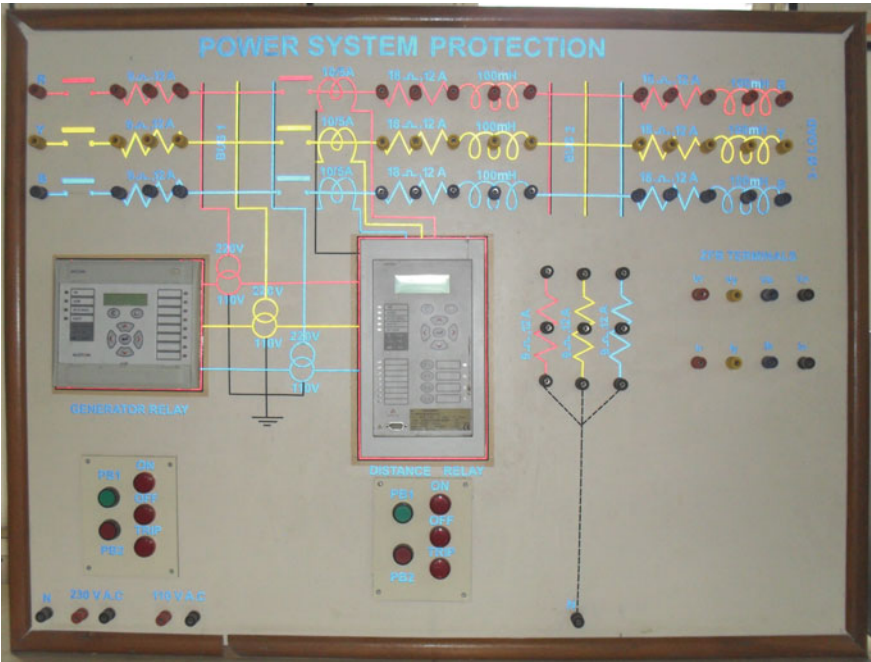


Fig. 2.8 An actual photograph of the experimental setup

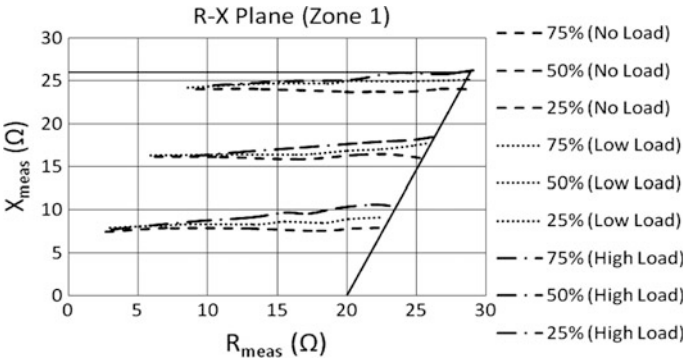
2.9.2 Results of Test Setup

Table 2.1 and Fig. 2.9 illustrate the performance of the conventional digital distance relay, covering 80 % of the complete line length in its first zone, for a high resistance single line-to-ground fault. The relay is set to include a fault resistance of 20 Ω in its first zone boundary, i.e.,  $R_{Fset} = 20\ \Omega$ .  $R_{Factual}$  is the maximum value of fault resistance that is actually incorporated by the conventional digital distance relay in its first zone boundary. The fault is considered at 25, 50, and 75 % of the line length for no-load and at other loading (low and high) conditions.

It is to be noted from Table 2.1 that the conventional digital distance relay provides satisfactory results for high resistance single line-to-ground faults during no-load conditions. However, for other loading conditions, its performance is highly affected by the presence of high resistance in the faulted path. Further, because of the variations in system and fault parameters, the error in the

**Table 2.1** Overreach/Underreach of conventional digital distance relay at different loading conditions

Fault location	Loading conditions	$R_{Fset}$ (Ω)	$R_{Factual}$ (Ω)	Over/underreach (%) $\left(\frac{R_{Factual}-R_{Fset}}{R_{Fset}} \times 100\%\right)$
25 %	No load	20	19.75	-1.25 %
	Low load	20	21.6	+8 %
	High load	20	23.5	+17.5 %
50 %	No load	20	19.65	-1.75 %
	Low load	20	21.4	+7 %
	High load	20	23.25	+16.25 %
75 %	No load	20	19.5	-2.5 %
	Low load	20	21.2	+6 %
	High load	20	23	+15 %



**Fig. 2.9** Effect of change in  $p$ ,  $R_F$ , and  $Z_{LD}$  on the impedance measured by the conventional digital distance relay

measurement of fault impedance given by the conventional relay increases. Figure 2.9 shows the adverse effects of increase of fault resistance and load in the measurement of fault impedance by the conventional digital distance relay.

## 2.10 Simulation Results

In this section, comparison of the conventional digital distance relaying scheme and the proposed algorithm for a high resistance single line-to-ground fault on 400 kV, 100 km transmission line is provided. The source and transmission line parameters are given in Appendix A. A single line-to-ground fault is simulated considering wide variations in fault location (0–80 % in steps of 20 %), power factor (0.7, 0.8 and 0.9), short-circuit capacity of source (5, 25 and 50 GVA), and fault resistance (0, 20, 40 and 60  $\Omega$ ). A load of 200 MVA having 0.8 power factor is assumed to be connected to the receiving end of the transmission line. In this section, the resistance and reactance measured by the conventional digital distance relaying scheme and the proposed algorithm are represented by  $R_C$ ,  $X_C$  and  $R_P$ ,  $X_P$ , respectively. The error occurred in the measurement of reactance by the conventional digital distance relaying scheme is represented as  $\varepsilon_{XC}$ . Similarly, the error occurred in the measurement of resistance and reactance by the proposed algorithm is represented as  $\varepsilon_{RP}$  and  $\varepsilon_{XP}$ , respectively. These errors are defined as follows:

$$\varepsilon_{XC} = \frac{X_C - X_{act}}{X_{act}} \times 100 \% \quad (2.13)$$

$$\varepsilon_{RP} = \frac{R_P - R_{act}}{R_{act}} \times 100 \% \text{ and } \varepsilon_{XP} = \frac{X_P - X_{act}}{X_{act}} \times 100 \% \quad (2.14)$$

It has been observed from the simulation results that there is a huge mismatch between the values of resistance ( $R_C$ ) measured by the conventional digital distance relaying scheme and the values of fault resistance ( $R_F$ ). Therefore, resistive errors ( $\varepsilon_{RC}$ ) of the conventional digital distance relay are not included in the results.

### 2.10.1 High Resistance Faults

Tables 2.2, 2.3, and 2.4 show the performance of the conventional digital distance relaying scheme and the proposed algorithm in terms of the error occurred in the measurement of resistance and reactance of the faulted portion of the transmission line. The results are obtained considering a single line-to-ground fault at different fault locations (0–80 % in steps of 20 %) with different values of fault resistance (0, 20, 40, and 60  $\Omega$ ).

**Table 2.2** Impedance measured by the conventional digital distance relaying scheme

$p$ (%)	$R_{\text{act}}$ ( $\Omega$ )	$X_{\text{act}}$ ( $\Omega$ )	$R_F = 0 \Omega$				$R_F = 20 \Omega$				$R_F = 40 \Omega$				$R_F = 60 \Omega$			
			$R_C$ ( $\Omega$ )	$X_C$ ( $\Omega$ )	$\varepsilon_{XC}$ (%)	$R_C$ ( $\Omega$ )	$X_C$ ( $\Omega$ )	$\varepsilon_{XC}$ (%)	$R_C$ ( $\Omega$ )	$X_C$ ( $\Omega$ )	$R_C$ ( $\Omega$ )	$X_C$ ( $\Omega$ )	$\varepsilon_{XC}$ (%)	$R_C$ ( $\Omega$ )	$X_C$ ( $\Omega$ )	$\varepsilon_{XC}$ (%)	$R_C$ ( $\Omega$ )	$X_C$ ( $\Omega$ )
0	0	0	0	0	—	0	0	—	10.35	0.067	—	20.49	0.22	—	30.43	0.45	—	—
20	0.6	6.66	0.77	6.62	−0.60	11.21	6.78	1.80	21.43	7.02	21.43	7.33	5.41	31.45	7.33	10.06	31.45	10.06
40	1.2	13.33	1.53	13.24	−0.68	12.07	13.49	1.20	22.4	13.82	22.4	14.23	3.68	32.51	14.23	6.75	32.51	6.75
60	1.8	20	2.29	19.86	−0.70	12.95	20.21	1.05	23.39	20.64	23.39	21.13	3.20	33.6	21.13	5.65	33.6	5.65
80	2.4	26.66	3.05	26.48	−0.68	13.84	26.94	1.05	24.4	27.47	24.4	28.07	3.04	34.73	28.07	5.29	34.73	5.29



**Table 2.3** Resistance measured by the proposed algorithm

$p$ (%)	$R_{act}$ ( $\Omega$ )	$R_F = 0 \Omega$		$R_F = 20 \Omega$		$R_F = 40 \Omega$		$R_F = 60 \Omega$	
		$R_P$ ( $\Omega$ )	$\varepsilon_{RP}$ (%)	$R_P$ ( $\Omega$ )	$\varepsilon_{RP}$ (%)	$R_P$ ( $\Omega$ )	$\varepsilon_{RP}$ (%)	$R_P$ ( $\Omega$ )	$\varepsilon_{RP}$ (%)
0	0	0.00	–	0.01	–	0.02	–	0.03	–
20	0.6	0.59	–1.15	0.60	–0.25	0.60	0.35	0.61	0.95
40	1.2	1.19	–1.22	1.19	–0.63	1.20	–0.33	1.20	–0.17
60	1.8	1.78	–1.30	1.79	–0.75	1.79	–0.50	1.79	–0.40
80	2.4	2.37	–1.38	2.38	–0.81	2.39	–0.51	2.39	–0.40

**Table 2.4** Reactance measured by the proposed algorithm

$p$ (%)	$X_{act}$ ( $\Omega$ )	$R_F = 0 \Omega$		$R_F = 20 \Omega$		$R_F = 40 \Omega$		$R_F = 60 \Omega$	
		$X_P$ ( $\Omega$ )	$\varepsilon_{XP}$ (%)	$X_P$ ( $\Omega$ )	$\varepsilon_{XP}$ (%)	$X_P$ ( $\Omega$ )	$\varepsilon_{XP}$ (%)	$X_P$ ( $\Omega$ )	$\varepsilon_{XP}$ (%)
0	0	0	–	0.065	–	0.201	–	0.38	–
20	6.66	6.59	–1.05	6.65	–0.15	6.69	0.45	6.73	1.05
40	13.33	13.17	–1.20	13.25	–0.60	13.29	–0.30	13.31	–0.15
60	20	19.74	–1.30	19.85	–0.75	19.9	–0.50	19.92	–0.40
80	26.66	26.3	–1.35	26.45	–0.79	26.53	–0.49	26.56	–0.38

It is to be noted from Table 2.2 that the conventional digital distance relaying scheme measures the correct value of impedance of the faulted portion of the transmission line for a low resistance single line-to-ground fault. However, as the value of fault resistance increases, the percentage error in the measurement of impedance of the faulted portion of the transmission line by the conventional digital distance relaying scheme increases. Conversely, it has been observed from Tables 2.3 and 2.4 that the percentage error in the measurement of resistance and reactance by the proposed algorithm remains within  $\pm 2\%$  for a single line-to-ground fault against wide variations in the fault resistance.

### 2.10.2 Sensitivity During Close-in Faults

The loci of fault impedance provided by the conventional digital distance relay and the proposed algorithm for a high resistance ( $R_F = 60 \Omega$ ) single line-to-ground fault at 3 % (close-in fault) from bus  $M$  is shown in Fig. 2.10.

It has been observed from Fig. 2.10 that the conventional digital distance relay sees a close-in fault outside its first zone boundary, which clearly indicates that the conventional digital distance relay is not able to sense close-in high resistance single line-to-ground faults. Conversely, the proposed algorithm measures the same fault in its first zone boundary (refer enlarged portion in Fig. 2.10). This clearly

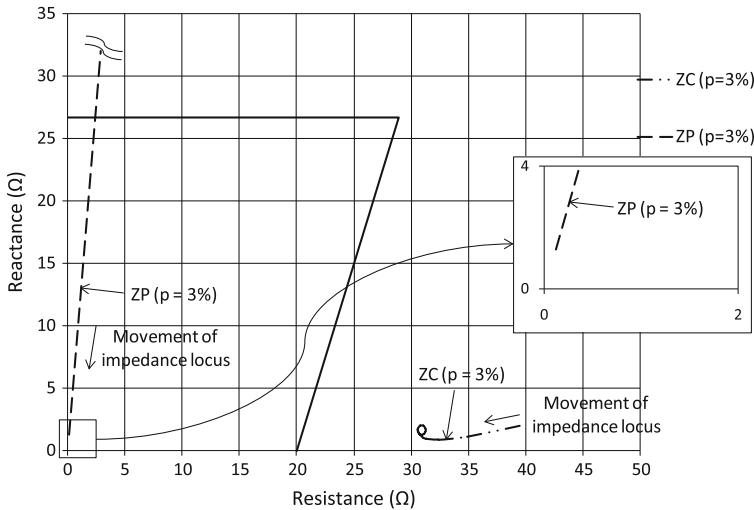


**Fig. 2.10** Impedance loci movement during close-in faults

reveals applicability of the proposed algorithm during close-in high resistance single line-to-ground faults.

### 2.10.3 Discrimination Between In-Zone and Out-Zone Faults

In order to check the effectiveness of the proposed algorithm for the remote end in-zone fault ( $p = 79\%$ ) and out-zone fault ( $p = 81\%$ ), a high resistance ( $R_F = 60\ \Omega$ ) single line-to-ground fault is considered. Figure 2.11 shows loci of the fault impedance provided by the conventional digital distance relaying scheme and the proposed algorithm for the aforementioned conditions.

It has been observed from Fig. 2.11 that the conventional digital distance relay measures the out-zone fault ( $p = 81\%$ ) outside its first zone boundary. However, it also measures the remote end in-zone fault ( $p = 79\%$ ) outside its first zone boundary; which is against the selectivity criteria of the protection system. Therefore, it can be concluded that the conventional digital distance relay is not able to provide effective discrimination between the remote end in-zone and out-zone faults. Whereas, referring to the enlarged portion of Fig. 2.11, it can be concluded that the proposed algorithm measures a high resistance single line-to-ground fault occurred at  $p = 79\%$  in its first zone boundary, and it sees the same type of fault occurred at  $p = 81\%$  outside its first zone boundary. Hence, the proposed algorithm is capable to provide discrimination between the remote end in-zone and out-zone faults correctly.

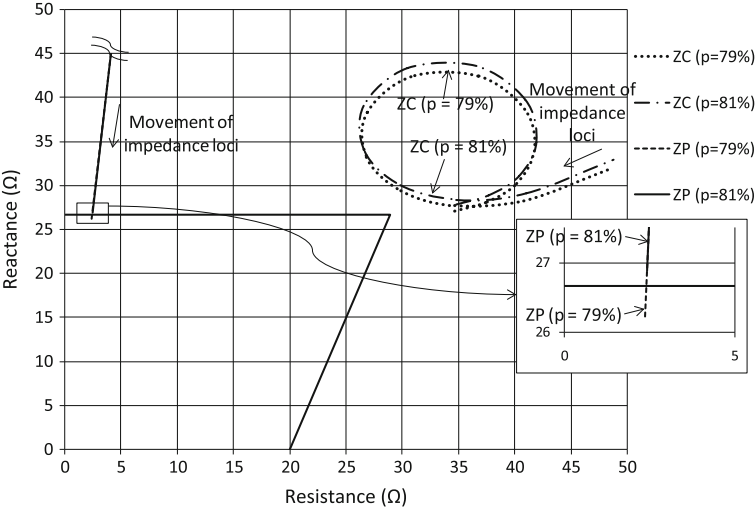


Fig. 2.11 Impedance loci movement during remote end faults

### 2.10.4 Effect of Variations in Short-Circuit Capacity of Source

Figure 2.12 shows the performance of the conventional digital distance relay and the proposed algorithm in terms of error in the measurement of impedance of the faulted portion of the transmission line for a high resistance ( $R_F = 60 \Omega$ ) single line-to-ground fault occurred on the line at different fault locations (0–80 % in steps

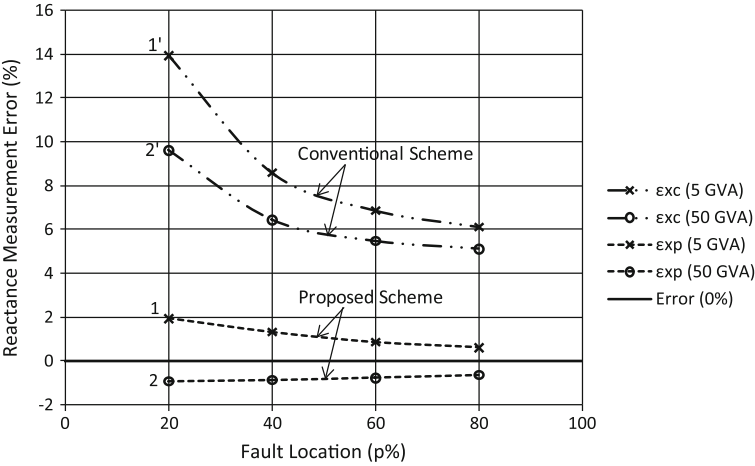


Fig. 2.12 Impedance measurement with different short-circuit capacity

of 20 %) having different short-circuit capacities of the three-phase source connected at the sending end. The bracketed values indicate short-circuit capacities (5 and 50 GVA) of source  $S$ .

It has been observed from Fig. 2.12 that as the short-circuit capacity of source  $S$  decreases from 50 to 5 GVA, the percentage error ( $\varepsilon_{xc}$ ) in the measurement of reactance provided by the conventional digital distance relay increases. Moreover, the percentage error ( $\varepsilon_{xc}$ ) is very high (increases sharply up to 14 %) for local end faults. Conversely, the percentage error ( $\varepsilon_{xp}$ ) in the measurement of reactance given by the proposed algorithm remains within a range of  $\pm 2$  % against the wide variations in short-circuit capacity of source  $S$  for all fault locations.

### 2.10.5 Effect of Change in Power Factor

Figure 2.13 shows the percentage errors,  $\varepsilon_{xc}$  and  $\varepsilon_{xp}$ , in the measurement of impedance of the faulted portion of the transmission line provided by the conventional digital distance relay and the proposed algorithm, respectively, for a high resistance ( $R_F = 60 \Omega$ ) single line-to-ground fault occurred at different fault locations (0–80 % in steps of 20 %) having two different values of power factor (0.7 and 0.9) of the load.

It is to be noted from Fig. 2.13 that for both values of power factor (0.7 and 0.9); the conventional digital distance relay measures the fault reactance with a large error (around 11 %). Further, for a low value of power factor (0.7), the percentage error ( $\varepsilon_{xc}$ ) increases sharply for local end faults. Conversely, the proposed algorithm measures fault reactance accurately for both values of power factor (the maximum percentage error is less than  $\pm 2$  %).

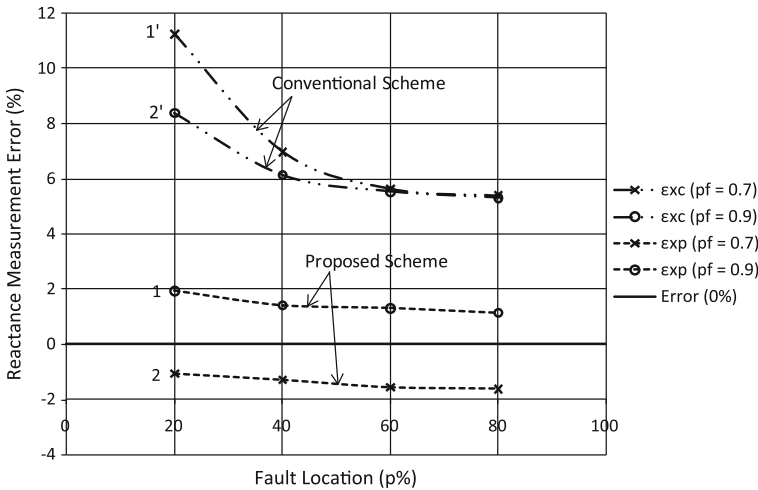


Fig. 2.13 Impedance measurement with different power factors

## 2.11 Advantages of the Proposed Algorithm

- (1) During a single line-to-ground fault, it is necessary to extend the first zone boundary of the conventional digital distance relay to incorporate high fault resistance. This is not at all required in the proposed algorithm.
- (2) The proposed algorithm is highly sensitive against close-in high resistance single line-to-ground faults.
- (3) Reach of the proposed algorithm is not affected by different loading conditions of line.
- (4) The proposed algorithm is capable to provide effective discrimination between the remote end in-zone and out-zone faults.
- (5) The proposed algorithm is highly accurate against wide variations in system and fault parameters, as it measures the fault impedance having percentage error within  $\pm 2\%$ .
- (6) The proposed algorithm is simple and having very less computational requirements.

## 2.12 Conclusion

A large number of online tests have been performed considering a single line-to-ground fault at various locations of a transmission line with different values of fault resistance, loading conditions, power factors and short-circuit capacities of source. It has been observed that the percentage error in the measurement of impedance of the faulted portion of the transmission line provided by the conventional digital distance relaying scheme is very high for high resistance single line-to-ground faults. In order to rectify these problems, a new digital distance relaying algorithm is proposed, which requires signals (voltages and currents) from local end data only. The proposed algorithm measures the correct values of resistance and reactance of the faulted portion of the transmission line with an accuracy of 98 % for high resistance single line-to-ground faults. Moreover, it also provides effective discrimination between remote end in-zone fault (79 %) and out-zone fault (81 %) occurred at the first zone boundary of a digital distance relay. In addition, it remains stable against the change in short-circuit capacity of source and variations in the power factor of the load by restricting the percentage error within  $\pm 2\%$ .

## References

1. ALSTOM Grid. Network protection & automation guide, edition May 2011, ISBN: 978-0-9568678-0-3
2. G. Ziegler, *Numerical Distance Protection: Principles and Applications* (Publicis Corporate Publishing, SEIMENS, 2008)

3. Protective Relay Engineers, Fundamentals of distance protection, 61st Annual Conference, 1–3 April 2008, College Station, TX, USA, pp. 1–34 (2008)
4. W.A. Elmore, *Protective Relaying Theory and Applications* (Marcel Dekker Inc., New York, 2004)
5. B.A. Oza, N.C. Nair, R.P. Mehta, V.H. Makwana, *Power System Protection and Switchgear* (Tata Mcgraw Hill, New Delhi, India, 2010)
6. B.R. Bhalja, R.P. Maheshwari, N.G. Chothani, *Protection and Switchgear* (Oxford Higher Education, India, 2011)
7. G. Gangadharan, P. Anbalagan, Microprocessor based three step quadrilateral distance relay for the protection of EHV/UHV transmission lines. *IEEE Trans. Power Deliv.* **7**(1), 91–97 (1992)
8. S.H. Horowitz, A.G. Phadke, *Power System Relaying* (John Wiley & Sons Ltd, England, 2008)
9. D.L. Waikar, A.C. Liew, S. Elangovan, Design, implementation and performance evaluation of a new digital distance relaying algorithm. *IEEE Trans. Power Syst.* **11**(1), 448–456 (1996)
10. H.J.A. Ferrer, I.D. Verduzco, E.V. Martinez, Fourier and walsh digital filtering algorithms for distance protection. *IEEE Trans. Power Syst.* **11**(1), 457–462 (1996)
11. H. Kudo, H. Sasaki, K. Seo, M. Takahashi, K. Yoshida, T. Maeda, Implementation of a digital distance relay using an interpolated integral solution of a differential equation. *IEEE Trans. Power Deliv.* **3**(4), 1475–1484 (1988)
12. M.M. Eissa, M. Masoud, A novel digital distance relaying technique for transmission line protection. *IEEE Trans. Power Deliv.* **16**(3), 380–384 (2001)
13. M.S. Sachdev, T.S. Sidhu, D.S. Ghotra, Implementation of an adaptive data window technique in a distance relay, in *IEE 7th International Conference on Developments in Power System Protection*, Amsterdam, 9–12th April 2001, pp. 161–164
14. T.S. Sidhu, D.S. Ghotra, M.S. Sachdev, A fast distance relay using adaptive data window filters. *Proc. IEEE Power Eng. Soc. Summer Meet.* **3**(16–20), 1407–1412 (2000)
15. T.S. Sidhu, D.S. Ghotra, M.S. Sachdev, An adaptive distance relay and its performance comparison with a fixed data window distance relay. *IEEE Trans. Power Deliv.* **17**(3), 691–697 (2002)
16. D.L. Waikar, S. Elangovan, A.C. Liew, Fault impedance estimation algorithm for digital distance relaying. *IEEE Trans. Power Deliv.* **9**(3), 1375–1383 (1994)
17. A.R. Van, C. Warrington, *Protective relays*, John Wiley & Sons Ltd. (1962)
18. S.W. Edmund, *Distance protection: Pushing the envelope*, Schweitzer Engineering Laboratories, Inc. (2006)
19. Y. Liao, S. Elangovan, Improved symmetrical component-based fault distance estimation for digital distance protection. *IET Gener. Transm. Distrib.* **145**(6), 739–746 (1998)
20. M.M. Eissa, Ground distance relay compensation based on fault resistance calculation. *IEEE Trans. Power Deliv.* **21**(4), 1830–1835 (2006)
21. V. Cook, Distance protection performance during simultaneous faults. *Proc. Inst. Electr. Eng.* **124**(2), 141–146 (1977)
22. M.E. Erezzaghi, P.A. Crossley, The Effect of high resistance faults on a distance relay. *IEEE Power Eng. Soc. Gen. Mee.* **4**, 2128–2133 (2003)
23. S. Jamali, H. Shateri, Robustness of distance relay with Mho characteristic against fault resistance, in *International Conference on Power System Technology, PowerCon*, 21–24th November 2004, Vol. 2, pp. 1833–1838 (2004)
24. Z.Y. Xu, S.J. Jiang, Q.X. Yang, T.S. Bi, Ground distance relaying algorithm for high resistance fault. *IET Gener. Transm. Distrib.* **4**(1), 27–35 (2010)
25. P. Ye, R.K. Li, D.S. Chen, A.K. David, A novel algorithm for high resistance earth fault distance protection, in *IEEE Proceedings—Transmission and Distribution Conference*, Los Angeles, CA, 15–20th September 1996, pp. 475–480
26. C.H. Kim, J.Y. Heo, R.K. Aggarwal, An enhanced zone 3 algorithm of a distance relay using transient components and state diagram. *IEEE Trans. Power Deliv.* **20**(1), 39–46 (2005)

27. K. El-Arroudi, G. Joos, D.T. McGillis, R. Brearley, Comprehensive transmission distance protection settings using an intelligent-based analysis of events and consequences. *IEEE Trans. Power Deliv.* **20**(3), 1817–1824 (2005)
28. S. Zhu, Y. Xing, F. Sui, Fault component reactance relay. *IEEE Trans. Power Deliv.* **11**(3), 1292–1300 (1996)
29. B.R. Bhalja, R.P. Maheshwari, High resistance faults on two terminal parallel transmission line: analysis, simulation studies and an adaptive distance relaying scheme. *IEEE Trans. Power Deliv.* **22**(2), 801–812 (2007)
30. E. Orduna, F. Garces, E. Handschin, Algorithmic-knowledge-based adaptive coordination in transmission protection. *IEEE Trans. Power Deliv.* **18**(1), 61–65 (2003)
31. K.H. Tseng, W.S. Kao, J.-R. Lin, Load model effects on distance relay settings. *IEEE Trans. Power Deliv.* **18**(4), 1140–1146 (2003)
32. K.K. Li, L.L. Lai, A.K. David, Stand alone intelligent digital distance relay. *IEEE Trans. Power Deliv.* **15**(1), 137–142 (2000)
33. S.A. Soman, T.B. Nguyen, M.A. Pai, R. Vaidyanathan, Analysis of angle stability problems: A transmission protection systems perspective. *IEEE Trans. Power Deliv.* **19**(3), 1024–1033 (2004)
34. S.H. Horowitz, A.G. Phadke, Third zone revisited. *IEEE Trans. Power Deliv.* **21**(1), 23–29 (2006)
35. S.M. Atif Saleem, A.M. Sharaf, A novel travelling wave based relaying scheme using wavelet transforms for arcing faults detection on series compensated transmission lines, *Electrical and Computer Engineering, CCECE 2007, Proceedings Canadian Conference*, 22–26th April 2007, pp. 575–578
36. A. Wiszniewski, Accurate Fault impedance locating algorithm, *IEE Proc. Gener. Transm. Distrib.* **130**(6), 311–315 (1983)
37. L. Eriksson, M.M. Saha, G.D. Rockefeller, An Accurate fault locator with compensation for apparent reactance in the fault resistance resulting from remote-end in-feed. *IEEE Trans. Power Apparatus Syst.* **PAS-104**(2), 424–436 (1985)
38. M.S. Sachdev, R. Agarwal, A technique for estimating transmission line fault locations from digital impedance relay measurements. *IEEE Trans. Power Deliv.* **3**(1), 121–129 (1988)
39. M.T. Sant, Y.G. Paithankar, Online digital fault locator for overhead transmission line. *Proc. Inst. Electr. Eng.* **126**(11), 1181–1185 (1979)
40. R. Kondow, Y. Sugiyama, M. Yamada, Microprocessor-based fault locator, in *IEE Conference Publication*, No. 249, pp. 188–192 (1985)
41. T. Takagi, Y. Yamakoshi, J. Baba, K. Uemura, T. Sakaguchi, A new algorithm of an accurate fault location for ehv/uhv transmission lines: Part 1—Fourier transformation method. *IEEE Trans. Power Apparatus Syst.* **PAS-100**(3), 1316–1323 (1981)
42. G.G. Richardson, O.T. Tan, An accurate fault location estimator for transmission lines, *IEEE Trans. Power Apparatus Syst.* **PAS-101**(4), 945–950 (1982)
43. A.D. Filomena, R.H. Salim, M. Resener, A.S. Bretas, Ground distance relaying with fault-resistance compensation for unbalanced systems. *IEEE Trans. Power Deliv.* **23**(3), 1319–1326 (2008)
44. Z. Zhizhe, C. Deshu, An adaptive approach in digital distance protection. *IEEE Trans. Power Deliv.* **6**(1), 135–142 (1991)
45. Y.Q. Xia, K.K. Li, A.K. David, Adaptive relay setting for standalone digital distance protection. *IEEE Trans. Power Deliv.* **9**(1), 480–491 (1994)
46. A.G. Jongepier, L. Van Der Sluis, Adaptive distance protection of a double-circuit line. *IEEE Trans. Power Deliv.* **9**(3), 1289–1297 (1994)
47. B.R. Bhalja, R.P. Maheshwari, An adaptive distance relaying scheme using radial basis function neural network. *Electr. Power Compon. Syst. Taylor & Francis* **35**(3), 245–259 (2007)
48. Q.K. Liu, S.F. Huang, H.Z. Liu, W.S. Liu, Adaptive impedance relay with composite polarizing voltage against fault resistance. *IEEE Trans. Power Deliv.* **23**(2), 586–592 (2008)

49. V.H. Makwana, B.R. Bhalja, A new digital distance relaying scheme for compensation of high-resistance faults on transmission line. *IEEE Trans. Power Deliv.* **27**(4), 2133–2140 (2012)
50. V. Terzija, Z. Radojevic, Numerical algorithm for adaptive autoreclosure and protection of medium voltage overhead lines. *IEEE Trans. Power Deliv.* **19**(2), 554–559 (2004)
51. C.R. Mason, *The Art and Science of Protective Relaying* (Wiley Eastern Limited, New Delhi, 1987)
52. V.H. Makwana, B.R. Bhalja, New digital distance relaying scheme for phase faults on doubly fed transmission lines. *IET Gener. Transm. Distrib.* **6**(3), 265–273 (2012)



Transmission Line Protection Using Digital Technology

Makwana, V.H.; Bhalja, B.R.

2016, XIX, 167 p. 62 illus., 1 illus. in color., Hardcover

ISBN: 978-981-10-1571-7